Feature-Enhanced Imaging With Compressed/Fractional SAR Systems

Inverse Problem Formalism and $\ell_2 - \ell_1$ Structured Descriptive Regularization Framework

Y.V. Shkvarko
Department of Electrical Engineering
CINVESTAV del IPN, Unidad Guadalajara
Guadalajara, Jalisco, Mexico
e-mail: shkvarko@gdl.cinvestav.mx

***Abstract*—We address a new technique for feature-enhanced radar imaging with compressed/fractional SAR data that unifies the descriptive experiment design regularization (DEDR) framework with the total variation (TV) image enhancement paradigm and the sparsity preserving regularizing projections onto convex solution sets (POCS). The new framework incorporates the ℓ_1 metric structured TV regularization into the ℓ_2 metric structured DEDR data agreement objective function and solves the overall reconstructive imaging inverse problem employing the POCD-DEDR-TV-restructured MVDR strategy.**

Keywords– compressed sensing; fractional SAR; regularization

I. INTRODUCTION

In low cost remote sensing (RS) missions with small airborne or unmanned flying vehicle platforms, low resolution sensors with simple and cheap hardware such as unfocused fractional SAR systems with onboard processors are attractive [1], [2]. However, the fractional synthesis mode inevitably sacrifices spatial resolution and usually suffers from harsh operational scenario uncertainties attributed to random signal perturbations in a turbulent atmosphere, imperfect system calibration, multiplicative speckle noise, and uncontrolled carrier trajectory deviations. All those make impossible wide focus aperture synthesis. That is why, all airborne fractional SAR systems employ the unfocused matched spatial filtering (MSF) method for image formation, sometimes referred to as a quick-look or compressed sensing mode [1–3]. The challenging problem is to post-process such low resolution speckle-corrupted MSF imagery aimed at accurate recovery of the scene power reflectivity map. The latter represents an estimate of the spatial spectrum pattern (SSP) of the backscattered field. Representing a spatial map of the RS scene power reflectivity (i.e., the second-order statistics of the random backscattered field), the SSP possesses the local spatial sparsity property for typical piecewise smooth scenes [3]. The problem is to reconstruct such SSP with considerable features enhancement, i.e., high estimation accuracy balanced over noise suppression.

In this study, we consider the inverse problem of feature-enhanced SSP reconstruction from the fractional/compressed SAR imagery stated and treated in a framework of the variational analysis (VA) inspired ℓ_1 metric structured regularization. The challenging proposition is to solve such the inverse problem with considerable resolution enhancement over noise suppression gains performed in a speeded-up iterative fashion. First, we resume the descriptive experiment design regularization (DEDR) framework [4,5] for solving the nonlinear uncertain inverse problem at hand based on the nonparametric ℓ_2 -type squared error norm minimization strategy robust against the operational uncertainties in the sense of the worst case statistical performance optimization [4]. Next, the DEDR framework is expanded by aggregating it with the SSP total variation (TV) minimization approach that exploits structural information on the desired image spatial gradient magnitude map sparsity over the RS scene [3], [6] and incorporates also the sparsity preserving projections onto convex sets (POCS) in the solution space with the user-specified/adaptive adjustments of the DEDR-, the TV- and the POCS-level degrees of freedom. Our method incorporates the ℓ_1 metric structured regularizing POCS-TV into the ℓ_2 metric structured DEDR data agreement objective function and solves the overall nonlinear radar image reconstruction inverse problem employing the POCS-DEDR-TV aggregated $\ell_2 - \ell_1$ restructured MVDR strategy [4,5]. We corroborate the effectiveness of our new POCS-DEDR-TV technique in the resolution enhancement over noise suppression gains with the guaranteed RS image gradient sparsity preservation via its comparison with other most prominent competing feature-enhanced radar imaging techniques in the literature [1–6].

II. INVERSE PROBLEM FORMALISM

The considered here SAR imaging inverse problem model is structurally similar to the previous studies [4–6]. Thus, in this section, we provide the problem background following the DEDR formalism [4,5] for convenience to the reader.

Following [5], consider the vector-form coherent equation of observation that relates the pixel-framed random scene reflectivity $\mathbf{v}$ with the fractional SAR trajectory data signal

$$\mathbf{u} = \tilde{\mathbf{S}}\mathbf{v} + \mathbf{n} = \mathbf{S}\mathbf{v} + \mathbf{\Delta}_{\mathbf{S}}\mathbf{v} + \mathbf{n} \qquad (1)$$

where $\mathbf{n}$ is the observation noise vector and $\tilde{\mathbf{S}} = \mathbf{S} + \mathbf{\Delta_S}$ is the $M \times K$ ($M < K$ for compressed sensing scenarios) matrix-form approximation of the integral perturbed signal formation operator (SFO), in which the regular component $\mathbf{S}$ is specified by the employed modulation and synthesis mode [4,5]. In (1), $\mathbf{v}$, $\mathbf{n}$, $\mathbf{u}$ are treated as Gaussian zero-mean vectors composed of the random entries $\{v_k\}_{k=1}^{K}$, $\{n_m\}_{m=1}^{M}$ and $\{u_m\}_{m=1}^{M}$, respectively [4,5]. These vectors are characterized by the correlation matrices, $\mathbf{R_v} = \mathbf{D}(\mathbf{b}) = \mathrm{diag}(\mathbf{b})$, the diagonal matrix with the vector-form SSP $\mathbf{b}$ at its principal diagonal, $\mathbf{R_n} = N_0\mathbf{I}$ and $\mathbf{R_u} = <\tilde{\mathbf{S}}\mathbf{R_v}\tilde{\mathbf{S}}^+> + N_0\mathbf{I}$, correspondingly, where the averaging $<\cdot>$ is performed over the randomness of perturbations $\mathbf{\Delta_S}$ of the regular SFO $\mathbf{S}$ in (1), superscript $^+$ stands for Hermitian conjugate, and N_0 is the white observation noise power. Vector $\mathbf{b}$ represents a lexicographically ordered by multi index $k = (k_x, k_y)$ vector-form approximation of the SSP map $\mathbf{B} = \{b(k_x, k_x)\}$ over the $K_y \times K_x$ pixel-framed 2-D scene $\{k_x = 1,\ldots, K_x;\ k_y = 1,\ldots, K_y;\ k = 1,\ldots, K = K_xK_y\}$ [1,4].

The feature-enhanced RS imaging problem at hand is to develop the framework (in this study, the unified POCS-DEDR-TV referred to as the $\ell_2 - \ell_1$ restructured robust MVDR method) and the related technique(s) for high-resolution estimation (feature-enhanced reconstruction) of the SSP

$$\hat{\mathbf{b}} = est_{\text{POCS-DEDR-TV}}\{\mathbf{b} \mid \mathbf{u} = \tilde{\mathbf{S}}\mathbf{v} + \mathbf{n}; \mathbf{R_u} = <\tilde{\mathbf{S}}\mathbf{D}(\mathbf{b})\tilde{\mathbf{S}}^+> + N_0\mathbf{I}\} \quad (2)$$

from the available recordings (1) of the complex (coherent) trajectory data $\mathbf{u}$ degraded by the composite noise (multiplicative $\mathbf{\Delta_S}$ and additive $\mathbf{n}$) with the SFO perturbation statistics $<\tilde{\mathbf{S}}\mathbf{R_v}\tilde{\mathbf{S}}^+>$ unknown to the observer.

To specify the piecewise SSP gradient map smoothness properties peculiar to the majority of the real-world RS scenes [3,6], we propose the variational analysis (VA) inspired metrics structure in the image space via inducing the following balanced anisotropic image norm and its gradient flow norm

$$\|\mathbf{b}\|_{\mathbb{B}_{(K)}} = m_{\ell_2}\Big(\sum_{k_x,k_y=1}^{K_x,K_y}(b(k_x,k_y))^2 + \sum_{k_x,k_y=1}^{K_x,K_y}(\nabla b(k_x,k_y))^2\Big)^{1/2} + m_{\ell_1}\,\|\,b(k_x,k_y)\,\|_{\ell_1}. \quad (3)$$

Here, the term with the weight factor m_{ℓ_2} specifies the equibalanced weighted image and image gradient ℓ_2-type norm. The second term with the weight factor m_{ℓ_1} induces the ℓ_1 structured image gradient norm component computed via the separable over x and y axes discrete-form finite differences $\|\nabla\mathbf{b}\|_{\ell_1} = ((\nabla_x b(k_x,k_y))^2 + (\nabla_y b(k_x,k_y)^2)^{1/2}$. This ℓ_1 metric conserves the image gradient piecewise sparseness properties [3,6]. Thus, the (3) induces the composite $\ell_2 - \ell_1$ structured image norm, in which the nonnegative user specified factors m_{ℓ_2} and m_{ℓ_1} control the balance between the two metrics measures. In this study, we use the equibalanced model $m_{\ell_2} = m_{\ell_1} = 1$. Nevertheless, other specifications are admissible [6].

III. DEDR Restructured Robust MVDR Technique

The high-resolution adaptive estimation of the SSP via the classical adaptive minimum variance distortionless response (MVDR) method [1] results in the solution-dependent strategy

$$\hat{b}_k = \frac{1}{\mathbf{s}_k^+\mathbf{R}_\mathbf{u}^{-1}(\mathbf{b})\mathbf{s}_k};\ k = 1,\ldots, K \quad (4)$$

optimal (in the MVDR sense) for the theoretical model-dependent ($\mathbf{b}$-dependent) covariance matrix inverse $\mathbf{R}_\mathbf{u}^{-1}(\mathbf{b})$ where $\mathbf{s}_k^+$ defines the so-called kth steering vector composed of the corresponding kth row ($k = 1,\ldots, K$) of the adjoint regular SFO matrix $\mathbf{S}^+$ [4]. In the real-world RS imaging scenarios, the unknown exact model of the covariance matrix $\mathbf{R_u}(\mathbf{b})$ is substituted by its sample maximum likelihood (ML) estimate [1] $\mathbf{Y} = \hat{\mathbf{R}}_\mathbf{u} = (1/J)\sum_{j=1}^{J}\mathbf{u}_{(j)}\mathbf{u}^+_{(j)}$ that yields the conventional MVDR estimation algorithm [1,4]

$$\hat{b}_k = \frac{1}{\mathbf{s}_k^+\mathbf{Y}^{-1}\mathbf{s}_k};\ k = 1,\ldots, K \quad (5)$$

feasible for the full rank $\mathbf{Y}$ only. From simple algebra, it is easy to corroborate that the theoretical model-based strategy (4) is algorithmically equivalent to the solution (with respect to the SSP vector $\mathbf{b}$) of the nonlinear equation

$$\{\mathbf{D}(\mathbf{b})\}_{\text{diag}} = \{\mathbf{W}^{(1)}\mathbf{R_u}\mathbf{W}^{(1)}\}_{\text{diag}} = \{\mathbf{W}^{(1)}(\mathbf{b})\mathbf{R_u}(\mathbf{b})\mathbf{W}^{(1)}(\mathbf{b})\}_{\text{diag}} \quad (6)$$

with the solution operator (SO of the 1st kind)

$$\mathbf{W}^{(1)} = \mathbf{W}^{(1)}(\mathbf{b}) = \mathbf{D}(\mathbf{b})\mathbf{S}^+\mathbf{R}_\mathbf{u}^{-1}(\mathbf{b}) \quad (7)$$

where as previously, $\mathbf{D} = \mathbf{D}(\mathbf{b}) = \mathrm{diag}(\mathbf{b})$ is the diagonal matrix composed of the SSP vector $\mathbf{b}$ at its principal diagonal. Referring to [4], the SO of the 1st kind (7) has its algorithmically equivalent counterpart (SO of the 2nd kind)

$$\mathbf{W}^{(2)} = \mathbf{W}^{(2)}(\mathbf{b}) = (\mathbf{S}^+\mathbf{R}_\mathbf{n}^{-1}\mathbf{S} + \mathbf{D}^{-1}(\mathbf{b}))^{-1}\mathbf{S}^+\mathbf{R}_\mathbf{n}^{-1}. \quad (8)$$

Substituting $\mathbf{W}^{(1)}$ in (6) by $\mathbf{W}^{(2)}$ and the theoretical covariance matrix $\mathbf{R_u}$ by its ML sample estimate $\mathbf{Y} = \hat{\mathbf{R}}_\mathbf{u}$ yields the DEDR-restructured MVDR strategy

$$\hat{\mathbf{b}} \to \text{solution to the Eq.} \to \{\mathbf{D}(\hat{\mathbf{b}})\}_{\text{diag}} = \{\mathbf{W}^{(2)}(\hat{\mathbf{b}})\mathbf{Y}\mathbf{W}^{(2)}(\hat{\mathbf{b}})\}_{\text{diag}} =$$

$$= \{\mathbf{A}(\hat{\mathbf{b}})\mathbf{Q}\mathbf{A}(\hat{\mathbf{b}})\}_{\text{diag}} \tag{9}$$

with the solution independent sufficient statistics matrix $\mathbf{Q} = \mathbf{S}^{+}\mathbf{Y}\mathbf{S}$ and the solution-dependent matrix-form reconstructive operator

$$\mathbf{A} = \mathbf{A}(\hat{\mathbf{b}}) = (\mathbf{D}(\hat{\mathbf{b}})\mathbf{\Psi} + N_0\mathbf{I})^{-1}\mathbf{D}(\hat{\mathbf{b}}) \,. \tag{10}$$

In (9), operator $\{\cdot\}_{\text{diag}}$ returns the vector of the principal diagonal of the embraced matrix, and in (10), $\mathbf{\Psi} = \mathbf{S}^{+}\mathbf{S}$ represents the matrix-form point spread function (PSF) of the so-called matched spatial filtering (MSF) linear low-resolution image formation system [1,4]. Note that matrix $\mathbf{A}$ does not involve the inversion of $\mathbf{D}(\hat{\mathbf{b}})$, hence, the constructed DEDR-restructured MVDR strategy (9) results in the desired sparsity preserving DEDR technique that admits zero entries in $\mathbf{b}$.

The DEDR framework [4] suggests the worst case statistical performances optimization approach to the problem at hand (2) with model uncertainties regarding the statistics of the SFO perturbations that yields the robust SO

$$\mathbf{W}^{(2)} = \mathbf{W}(\hat{\mathbf{b}}) = \mathbf{A}(\hat{\mathbf{b}} \mid N_{\Sigma})\mathbf{S}^{+} = (\mathbf{D}(\hat{\mathbf{b}})\mathbf{\Psi} + N_{\Sigma}\mathbf{I})^{-1}\mathbf{D}(\hat{\mathbf{b}})\mathbf{S}^{+} \tag{11}$$

in which $N_{\Sigma} = N_0 + \beta$ is the observation noise power N_0 augmented by factor $\beta \geq 0$ adjusted to the regular SFO Loewner ordering factor and the statistical uncertainty bound for the SFO perturbations (see [4] for details). Hence, the robust modification of the DEDR is now constructed simply by replacing in (9), (10) N_0 by the composite (loaded) $N_{\Sigma} = N_0 + \beta$. In practical estimation scenarios, the diagonal loading factor β can be evaluated empirically from the speckle-corrupted low-resolution MSF image following one of the local statistics methods exemplified in [4,6].

Next, we adapt the robust sparsity preserving DEDR (9), (10) to the considered here single look fractional SAR mode (J = 1) substituting $\mathbf{Y}$ by $\mathbf{u}\mathbf{u}^{+}$ and defining the complex MSF imaging system output

$$\mathbf{q} = \mathbf{S}^{+}\mathbf{u} \tag{12}$$

in which case, the robust sparsity preserving DEDR strategy (9) yields the solution in the form of the elementwise square detected (SQ-DET$\{\cdot\}$) output of the solution-dependent reconstructive operator $\mathbf{A}(\hat{\mathbf{b}})$ applied to $\mathbf{q}$

$$\hat{\mathbf{b}} \rightarrow \text{solution to the Eq.} \rightarrow \hat{\mathbf{b}} = \text{SQ-DET}\{\mathbf{A}(\hat{\mathbf{b}})\mathbf{q}\} =$$
$$= \{\mathbf{A}(\hat{\mathbf{b}})\mathbf{q}\mathbf{q}^{+}\mathbf{A}^{+}(\hat{\mathbf{b}})\}_{\text{diag}} \,. \tag{13}$$

The next stage of our design consists in incorporating the convergence guaranteed POCS operator $\mathcal{P}$ into the solver for (13) that yields the resulting POCS-regularized DEDR-TV (POCS-DEDR-TV) technique in the form of a solution to the nonlinear equation

$$\hat{\mathbf{b}} = \mathcal{P}\{\mathbf{A}(\hat{\mathbf{b}})\mathbf{q}\mathbf{q}^{+}\mathbf{A}^{+}(\hat{\mathbf{b}})\}_{\text{diag}} \tag{14}$$

with $\mathbf{A} = \mathbf{A}(\hat{\mathbf{b}})$ specified by (10) and the composite POCS operator $\mathcal{P} = \mathcal{P}_2\mathcal{P}_1$. The action of such $\mathcal{P}$ is twofold. First, operator $\mathcal{P}_1$ transforms (14) into the corresponding implicit contractive mapping iterative scheme that preserves the imposed metric structure (3) in the solution space $\mathbb{B}_{(K)}$ [6]. Second, $\mathcal{P}_2$ acts as a hard thresholding operator that at each iteration i = 1, … clips off all entries of $\hat{\mathbf{b}}_{[i]}$ lower than the user prescribed positive sparsity preserving tolerance threshold. Hence, such $\mathcal{P} = \mathcal{P}_2\mathcal{P}_1$ serves as a convergence guaranteed composite POCS operator [5,6]. The iterative process is initialized with the standard low-resolution MSF (zero-step iteration) image $\hat{\mathbf{b}}_{[0]} = \{\mathbf{q}\mathbf{q}^{+}\}_{\text{diag}}$ and is terminated at $\hat{\mathbf{b}}_{[I]}$ for which the conventional 0.1% ℓ_2 squared norm error tolerance convergence level is attained at some $i = I$.

Last, to construct the speeded up computational structure of the iterative-form version of the POCS-DEDR-TV technique (14) we make the use of the operator feedback loop structure of Fig. 1 that yields the composite transfer matrix

$$\mathbf{A} = (\mathbf{A}_1\mathbf{A}_2 + k\mathbf{I})^{-1}\mathbf{A}_1 \,. \tag{15}$$

With the specifications, $k = N_{\Sigma}$, $\mathbf{A}_1 = \mathbf{D}(\hat{\mathbf{b}}_{[i]})$ and $\mathbf{A}_2 = \mathbf{\Psi}$, this scheme is exactly suited to performs the computing required by the solver (13) at the coherent data processing level. The computational structure of the resulting iterative-form POCS-DEDR-TV technique (14) is presented in Fig. 2.

IV. Simulations and Discussions

Figs. 3, 4 report some qualitative results of enhancement of a fractional SAR image applying different DEDR-related techniques. The test 512×512 pixel-format high resolution scene of Fig. 3 borrowed from the real-world SAR imagery [7] relates to the hypothetical full focused SAR imaging mode. The low resolution speckle corrupted radar image of the same scene presented in Fig. 4(a) corresponds to the single look fractional SAR mode (quick look fractional SAR modality) for

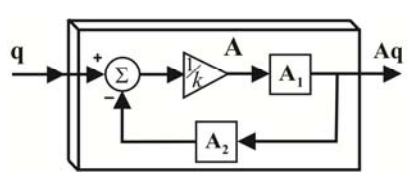

Figure 1. Feedback loop structure of operator **A** defined by (15).

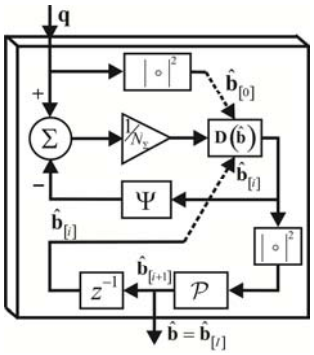

Figure 2. Double feedback loop-type implicit iterative contractive mapping algorithmic structure of the sparsity preserving POCS-DEDR-TV technique (14). Block labeled by z^{-1} defines the one iteration step delay operator.

Figure 3. Test 512×512-pixel scene (not observable with the fractional SAR system under consideration) borrowed from the real-world SAR imagery [7]).

the typical operational scenario specifications, the same as in the comparative previous studies [5,6] as specified in the Figure captions. Figs. 4(b) thru Fig. 4(f) report the feature-enhanced radar imaging results obtained with different compared DEDR-related techniques specified in the Figure captions. These results corroborate that the best perceptual fractional SAR image enhancement performances as well as quantitative enhancement measures and convergence rates (compared to those reported in the related study [6] for the most prominent competing methods in the literature) are attained with the developed POCS-DEDR-TV technique (14).

REFERENCES

[1] D.R. Wehner, *High-Resolution Radar*, 2nd ed., Boston, MA: Artech House, 1994.

[2] *Principles and Applications of Imaging Radar*, *Manual of Remote Sensing*, 3d ed., F.M. Henderson and A.V. Lewis, Eds., vol. 3, NY: Willey, 1998.

[3] V.M. Patel, G.R Easley, D.M. Healy, and R. Chellappa, "Compressed synthetic aperture radar", *IEEE Journal of Selected Topics in Signal Proc*., vol. 4, pp. 244-254, April 2010.

[4] Y.V. Shkvarko, "Unifying experiment design and convex regularization techniques for enhanced imaging with uncertain remote sensing data —Part I: Theory; —Part II: Adaptive implementation and performance issues", *IEEE Trans. Geoscience and Remote Sensing*, vol. 48, No. 1, pp. 82-111, Jan. 2010.

[5] Y.V. Shkvarko., J. Tuxpan, and S.R.. Santos, "Dynamic experiment design regularization approach to adaptive imaging with array radar/SAR sensor systems", *Sensors*, vol. 11, pp 4483-4511, Apr. 2011.

[6] Y.V. Shkvarko, J. Tuxpan, and S.R. Santos, " $\ell_2-\ell_1$ structured descriptive experiment design regularization based enhancement of fractional SAR imagery", *Signal Processing*, Vol. 2013, http://dx.doi.org/10.1016/j.sigpro.2013.03.024, (in press), July 2013.

[7] "TerraSAR-X" imagery, *Available at*: http://www.astrium-geo.com/es/570-galeria-de-imagenes?img

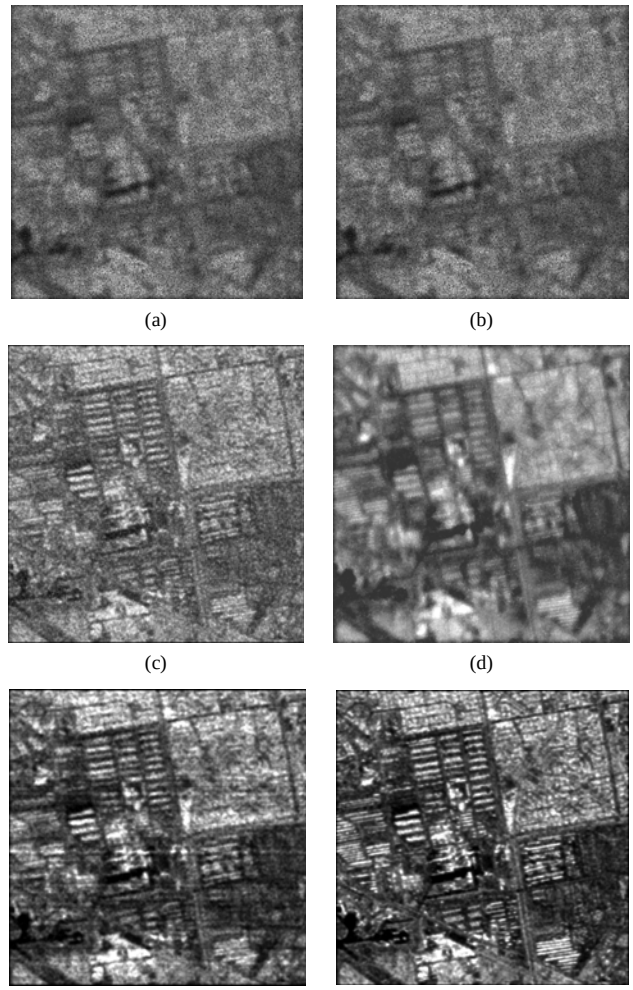

Fig. 4. Simulation results of the fractional SAR imaging experiment: (a) 512×512 pixel-framed low resolution speckle corrupted MSF image of the scene of Fig.3 formed with a simulated fractional SAR system (modeled fractional SAR system parameters: triangular range point spread function (PSF) width (at ½ of the peak value) κ_r = 15 pixels; Gaussian bell azimuth PSF width (at ½ of the peak value) κ_a = 30 pixels; worst case single-look scenario with fully developed speckle, SNR = 0 dB); (b) image despeckled applying the DEDR-related local statistics-based anisotropic diffusion technique [5]; (c) image enhanced applying the VA-free DEDR method [4] (convergence at I = 20 iterations); (d) image enhanced with the TV-inspired ℓ_1 only structured DEDR method [5] (convergence at I = 15 iterations); (e) image enhanced using the most competing $\ell_2-\ell_1$ structured dynamic DEDR-VA technique [6] that does *not* employ the POCS-DEDR-TV-restructured MVDR strategy (convergence at I = 9 iterations); (f) image enhanced applying the developed here POCS-DEDR-TV-restructured MVDR method (14) with the zero threshold level in the POCS operator $\mathcal{P}_2=\mathcal{P}_+$, a projector onto the positive convex cone set (convergence at I = 4 iterations).